ChemComm

Accepted Manuscript

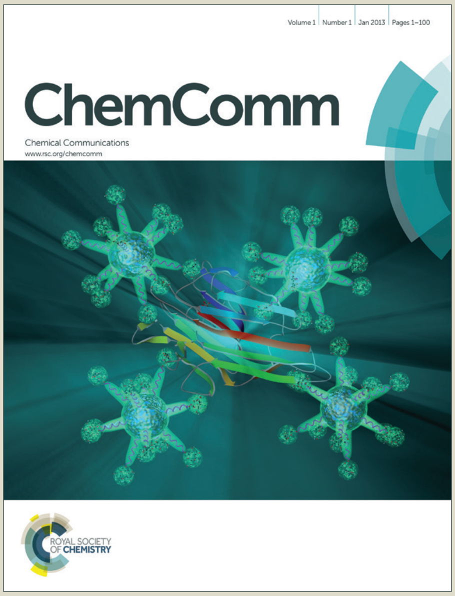

ROYAL SOCIETY OF CHEMISTRY

www.rsc.org/chemcomm

Journal Name

COMMUNICATION

pH triggered superior selective adsorption and separation of both the cationic and anionic dyes and photocatalytic activity on fully exfoliated titanatelayer–natural polymer based nanocomposite

Received 00th January 20xx,
Accepted 00th January 20xx

DOI: 10.1039/x0xx00000x

www.rsc.org/

Amit Kumar Sarkar,[a] Arka Saha,[b] Asit Baran Panda,*[,b] Sagar Pal*[,a]

Fully exfoliated titanate layer–natural polymer amylopectin based nanocomposite, with pH responsive superior selective adsorption, separation of both the cationic (MB: 599 mg.g^{-1} at pH 9) and anionic (MO: 558 mg.g^{-1} at pH 3) dyes and photo degradation properties, have been realized through simultaneous *in-situ* layered titanate formation, exfoliation and polymerization.

Highly toxic dyes are one of the major contributor of present water pollution and became serious threat to human health.[1] However, these dyes are crucial in different chemical, textile, printing and even biotechnology industries. Thus, efficient removal of dyes from pollutant water by reliable, cost-effective and eco-friendly techniques is very important. Separation through adsorption is attractive and mostly used method, as the process is simple and economical.[2] Sometimes, the total removal of dyes or their intermediate was not required, as some important intermediate needs to be recycled or separation of only targeted dye is needed.[3] Thus, development of efficient advanced adsorbent, which is able to adsorb and separate specific dye selectively, is essential and consider to be challenging.

Last few years, the exploration of novel selective adsorbent has got stimulated and to date, numbers of promising adsorbents, with selective adsorption ability, have been developed which includes, supramolecular hydrogels,[4] polymers,[5] organic-Inorganic hybrid,[6] modified graphene oxide and/or carbon nanotube[7] and inorganic nanostructured[8] materials. Most of these adsorbents are selective towards only one type of dye (either cationic or anionic), and the adsorption efficiency is not satisfactory and adsorbents are costly. Here it is essential to emphasize that adsorbents, which are capable to adsorb both the cationic or anionic dye selectively by changing the adsorption conditions are highly desirable and very rarely reported. Sarkar *et al*. reported pH trigger selective adsorption of cationic methyl violet and anionic methyl orange using modified graphene-carbon nanotube hybrid with low adsorption efficiency (294 mg g^{-1} of MO).[7a] Further, decomposition of adsorbed undesired dyes and their intermediates are another issue and most of the developed selective adsorbents are not capable to degrade the adsorbed dye and need additional step.

Among the developed selective and non-selective adsorbents, modified natural polymers appear to be the better option with respect to the adsorption efficiency, availability and cost effectivity.[5,9] However, adsorption efficacy of these modified natural polymers are not satisfactory. In the recent-past, the organic-inorganic hybrid polymeric nanocomposites have received great interest as they show improved properties, including adsorption efficiency, sometimes impart additional functionality through synergism in guest-host interaction.[10,11] Further, it is reported that cheap and abundant Layered titanates are also demonstrated efficient selective adsorption, photocatalytic property.[8a-b] Thus, it is expected that the combination of two i.e. nanocomposite of titanate layered and modified natural polymer, supposed to be the novel selective adsorbent with photocatalytic property. However, exfoliation of titanate layers are the main hurdle, due to its high charge density (1.07) compared to its "*closest of kin*" layered silicates (0.33).[12] In-turn, there are very few reports on layered titanate based polymeric composites.[13] Most of the reported procedures are based on the exfoliation of layers through intercalation of cationic surfactant through ion exchange followed by polymer incorporation. Thus, direct polymer-titanate sheet interaction is negligible and the layers are not fully exfoliated.

Herein, we report the direct synthesis of nanocomposite [*exf*.LT/AP-g-p(DEAEMA)] comprise of fully exfoliated layered titanate and amino functionalized natural polymer amylopectin [i.e. *poly*(2-diethylamino) ethyl methacrylate grafted amylopectin, AP-g-*p*(DEAEMA)]. Synthesis of nanocomposite was performed in one step and the strategy is based on simultaneous *in-situ* formation, exfoliation of layered titanate, and polymerization, using aqueous titanium peroxo carbonate complex solution as precursor[8a-b] (see ESI[†], detailed synthetic procedure). The adopted strategy is novel and reporting for the first time. To our delight, the synthesized

---

[a.] *Polymer Chemistry Laboratory, Department of Applied Chemistry, Indian School of Mines, Dhanbad-826004, India. Tel: 91-326-2235769; Fax: 91-326-2296615, E-mail: sagarpal1@hotmail.com, web:sites.google.com/site/drsagarpalism/*

[b.] *Discipline of Inorganic Materials and Catalysis, Central salt and Marine Chemicals Research Institute (CSIR), Bhavnagar-364002, Gujarat, India, E-mail: abpanda@csmcri.org, web: http://abpandasgroup.webs.com*

Electronic Supplementary Information (ESI) available: [synthetic procedure, Chemcterization figures and results, dye adsorption, regeneration by desorption and photocatalytic degradation results]. See DOI: 10.1039/x0xx00000x nanocomposite showed improved pH triggered dye adsorption property, adsorbed cationic dye methylene blue (MB) or malachite green (MG) selectively at pH 8-9, and anionic methyl orange (MO) and reactive black (RB) selectively at pH 3, with improved adsorption efficiency (Q_{max}, MO: 558.65 mg.g^{-1} and RB: 598.80 mg.g^{-1}) compared to reported adsorbents. The adsorbent is easily regenerable through both the desorption and photocatalytic degradation of adsorbed dye.

The synthetic strategy is based on the grafting of (2-diethylamino) ethyl methacrylate on amylopectin backbone by simple radical polymerization mechanism at 80°C [AP-g-p(DEAEMA)] (Table S1, see ESI[†]) in presence of peroxo titanium carbonate complex, potassium persulfate as initiator. During the reaction, controlled decomposition/hydrolysis of titanium precursor took place and formed negatively charged TiO_6 octahedra.[8a-b] With increase in reaction time, the degree of polymerization as well as grafting increased simultaneously. Besides, the TiO_6 octahedra polymerized one dimensionally to give sheet structure, where the negatively charged titania sheet was stabilized by cationic polymer and restrict the self-stacking (Scheme 1). Thus in the synthesis, use of cationically modified copolymer makes advantageous as it stabilized the newly formed negatively charged titanate layers by its ammonium group through ion interaction, restricts the stacking and ensures straight forward exfoliated titanate sheets-polymer interaction. Use of amylopectin, an easily available, low cost and more importantly biodegradable naturally occurring branched polysaccharide, makes the procedure advantageous and acceptable. For comparison, we have also synthesized *ex-situ* CTAB *exf*.LT incorporated graft copolymer (CTAB *exf*.LT/AP-g-p(DEAEMA) as well as *ex-situ* pre-formed layered titanate incorporated nanocomposite *LT*/AP-g-p(DEAEMA).

In the solid state ^{13}C NMR spectrum of grafted polymer AP-g-p(DEAEMA), the presence of additional peaks with respect to corresponding bare AP confirmed the formation of graft copolymer (Fig. S1, see ESI[†]). Whereas, in the ^{13}C NMR spectrum of corresponding composite [*exf*.LT/AP-g-p(DEAEMA)], all the downfield shifted characteristics peaks of bare graft copolymer was observed due to the electrostatic interactions between anionic titanate sheet and cationic AP-g-p(DEAEMA), which confirmed the formation of titanate layer- graft copolymer composite with good interaction (Fig. S1, see ESI[†]). Similarly, the FTIR spectra of graft copolymer and nanocomposite depict the successful grafting and formation of respective titanate composite (Fig. S2, see ESI[†]). FESEM analysis indicates the drastic change in surface morphology of AP-g-p(DEAEMA) from fibrillar to porous micro round shaped clusters during nanocomposite formation (Fig. S3, see ESI[†]). AFM images depict the formation of granular topography and support the SEM results (Fig. S4, see ESI[†]). Presence of titanium in the EDAX spectra of *exf*.LT/AP-g-p(DEAEMA) also confirmed the incorporation of titanate sheet in composite (Fig. S5, see ESI[†]). TGA analysis suggested the enhancement of thermal stability after formation of *exf*.LT/AP-g-p(DEAEMA) nanocomposite (Fig. S6, see ESI[†]).

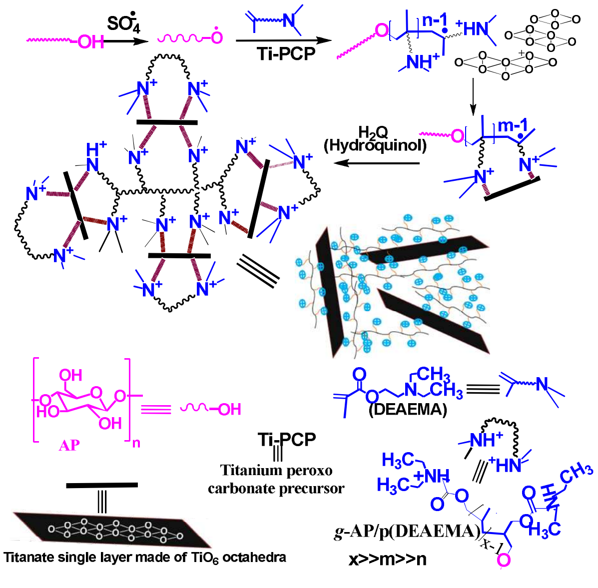

Scheme 1. Schematic representation for the synthesis of fully exfoliated titanate layered- AP-g-p(DEAEMA) nanocomposite i.e. *exf*.LT/AP-g-p(DEAEMA).

The XRD pattern of the layered titanate synthesized in absence of polymer can be indexed to protonic titanate $H_2Ti_2O_5$-H_2O, with interlayered spacing of 0.95 nm (2θ=9.7) [Fig. 1a (i)]. While in the XRD pattern of *exf*.LT/AP-g-p(DEAEMA) composite, presence of all other peaks of titanate, with low intensity, except the peak at 2θ=9.7, responsible for stacked titanate layer, indiactes the presence of unstacked titanate sheets, i.e. exfoliated in the composite [Fig. 1a(ii),Fig. S7, see ESI[†]]. In the XRD pattern of *LT*/AP-g-p(DEAEMA) composite, the presence of intense diffraction peak for layered structure (2θ=9.7) along with other peaks indicates that stacked layer structure remained intact [Fig. 1a (iii)]. TEM image of pure titanate confirm the presence of stacked titanate layers with inter layered distance of 0.84 nm (Fig. S8, see ESI[†]). In the low resolution TEM image of the *in-situ* formed *exf*.LT/AP-g-p(DEAEMA) composite, homogeneously distributed randomly oriented wire like structure, titanate layers, were observed (Fig. 1b, and Fig. S9, see ESI[†]), which are absent in the TEM image of pure graft copolymer (Fig. S10, see ESI[†]). Magnified image of composite depicts the distinctly identifiable randomly oriented and homogeneously distributed individual sheets throughout the polymer (Fig. 1c). In HRTEM image, the titanate layer lying in the outward of composite surface (Fig. 1d) as well as on the head of the layer as observed as wire like (inset Fig.1d & Fig. S11, see ESI[†]) suggests the presence of distinct lattice fringes in the inter planer distance of 0.23 and 0.38 nm, respectively. This confirmed the presence of highly crystalline exfoliated titanate layer in composite.

The synthesized *exf*.LT/AP-g-p(DEAEMA) nanocomposite was used as adsorbent for separation of both cationic (methylene blue, MB and Malachite green, MG) and anionic (methyl orange, MO and reactive black, RB) pollutant dyes (Structure of respective dyes are shown in Fig. S12, see ESI[†]) from their corresponding aqueous solution. Extent of adsorption rate and efficiency were optimized by varying the parameters like pH, temperature, adsorbent dosage, dye concentration, contact time of solution (Fig. S13-S17, see ESI[†]) by monitoring the UV-vis adsorption spectrscopy. It was observed that anionic dye adsorption efficiency of composite was decreased with increase in pH from 3, where as for cationic dyes the adsorption efficiency was increased with increase in pH and

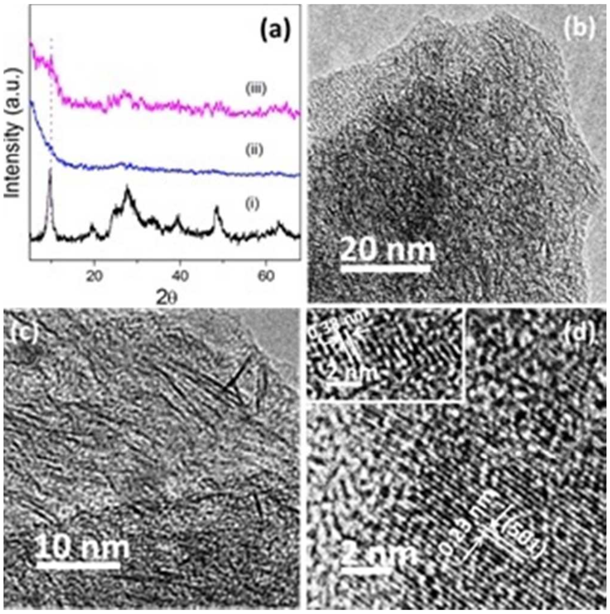

Fig.1.(a) XRD pattern of pure layered titanate (i), *in-situ* exfoliated*exf*.LT/AP-g-p(DEAEMA) composite (ii), *ex-situ* synthesized *LT*/AP-g-p(DEAEMA) composite and (b-d) the TEM and HR-TEM images of *in-situ* exfoliated*exf*.LT/AP-g-p(DEAEMA) composite.

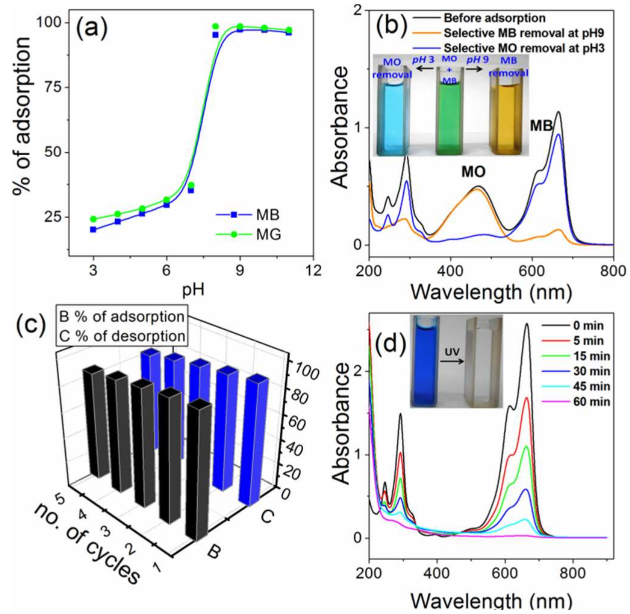

Fig. 2. Effect of pH on % adsorption of cationic dye (MB & MG); (b) pH selective adsorption of cationic (MB) and anionic (MO) dyes from the mixed solution and the corresponding photograph in inset; (c) extent of regeneration of adsorption efficiency through desorption up to 5 cycles for MB and (d) photocatalytic regeneration of water suspended composite by UV light irradiation.

maximum efficiency was obtained within pH 8-9 (Fig. 2a & Fig. S13, see ESI[†]). In the optimized conditions, the maximum anionic dye adsorption values: for MO (Q_{max})- 558.65 mg.g^{-1} and for RB (Q_{max}): 598.80 mg.g^{-1} at pH 3 and cationic dyes adsorption values: MG (Q_{max})- 380.22 mg.g^{-1} and MB (Q_{max})- 598.80 mg.g^{-1} at pH 8-9 were realised. In the control adsorption experiments, pure graft copolymer i.e. AP-g-p(DEAEMA) showed very low adsorption capacity. Although both the CTAB *exf*.LT/AP-g-p(DEAEMA) and LT/AP-g-p(DEAEMA) composites showed pH selective adsorption property with enhanced adsorption efficiency as compared to AP-g-p(DEAEMA), however the efficiency was reasonably low than that of *exf*.LT/AP-g-p(DEAEMA) nanocomposite (Table S2,see ESI[†]).

All the above mentioned experimental findings indicate the presence of pH triggered selective cationic or anionic adsorption property of the synthesized nanocomposite. Selective adsorption of MO at pH 3 and MB at pH 9 from the mixed solution of MO & MB as well as selective removal of MO at pH 3 and MG at pH 8 from the mixed solution of MO & MG confirmed that the synthesized nanocomposite is capable to adsorb one dye selectively from mixture (Fig. 2b and also Fig. S18, see ESI[†]).

Now, it is essential to identify the origin and exact mechanism for such high pH selective adsorption efficiency of *exf*.LT/AP-g-p(DEAEMA) nanocomposite. The adsorption efficiency of an adsorbent is highly dependent on its surface area, and selectivity is dependent on its surface charge. Calculated total surface area of *exf*.LT/AP-g-p(DEAEMA) is much higher than that of CTAB *exf*.LT/AP-g-p(DEAEMA), LT/AP-g-p(DEAEMA) and AP-g-p(DEAEMA) (Table S2, and Fig. S19, see ESI[†]). This indicates that on incorporation of individual titanate layers in the polymer, the surface area was increased through polymer titanate sheet interaction. The surface area of CTAB *exf*.LT/AP-g- p(DEAEMA) is quite low than that of *exf*.LT/AP-g-p(DEAEMA), although the exfoliated layers are present in the polymer matrix. This is most probably due to the presence of CTAB in the titanate layer surface, which restricts direct polymer-titanate interaction, and *in-turn* the surface area.

Evaluation of surface charge through zeta potential calculation indicates that the point to zero charge (pH_{pzc}) of the composite i.e. *exf*.LT/AP-g-p(DEAEMA) is 4.4 (Fig. S20, see ESI[†]). Thus, the composite carries positive surface charges at pH<4.4, while the composite demonstrates negative surface charges beyond pH 4.4. Therefore in acidic pH, electrostatic attraction between cationically charged adsorbent with anionic MO and RB is primarily responsible for removal of these dyes. While, in alkaline pH, the attractive interactions between anionic adsorbent with cationic MB and MG is accountable for the removal of cationic dyes. At acidic media, polymer chains of *exf*.LT/AP-g-p(DEAEMA) composite were highly stretched owing to electrostatic interactions with fully exfoliated single titanate sheet and covered up the sheets. Thus, intractable area of positively charged polymer chains was increased for an efficient adsorption process. Therefore, the stretched AP-*g*-p(DEAEMA) polymer chains on single sheet of titanate could hold excess amount of anionic RB/MO dyes. But at pH>4.4, the stretched protonated chain of AP-*g*-p(DEAEMA) became deprotonated. So, the stretched confirmation of *poly*(DEAEMA) was collapsed followed by negatively charged titanate sheets are free to bind with cationic dyes (MB, MG) and the efficient adsorption took place through ion interaction. To support the prediction, we have calculated the hydrodynamic diameter of the adsorbent in two different pH. The obtained hydrodynamic diameter of 1699 nm at pH 3 and 377 nm at pH 9 (Table S3 and Fig. S21, see ESI[†]), confirmed that the *poly* (DEAEMA) chains present in the composite became protonated, swelled and repulsive interactions predominate in acidic media, which results in the increase in hydrodynamic diameter. While in basic media, the stretched confirmation of *poly* (DEAEMA) chains were collapsed, and resulted the reduction of hydrodynamic diameter.[14] So, due to the absence of titanate layers in the pure AP-g-p(DEAEMA) polymer, the accessible surface area was less and in-turn the anionic dye adsorption efficiency was very low and cationic dye adsorption efficiency is negligible. The extent of adsorption on LT/AP-g-p(DEAEMA) were increased compared to pure AP-g-p(DEAEMA) polymer due to the incorporation of titanate sheet, but it is much less than that of *exf*.LT/AP-g-p(DEAEMA). This is mainly because of the less extent of polymer-titanate sheet intractable area and accessible sheet surface due to the stacking of titanate sheet. Besides, the FESEM images of dye loaded nanocomposite predict that surface adsorption took place (Fig. S22, see ESI[†]). The dye sorption process is in agreement with pseudo second order and Langmuir isotherm models (Fig. S23-S24, Table S4-S6, see ESI[†]). Further, the sorption process is also thermodynamically favourable (Fig. S25, Table S7, see ESI[†])

Isolation of adsorbed dye or decomposition of unwanted dye and regeneration of adsorbent are other important issues for a good adsorbent. To our delight, the adsorbed dyes were efficiently isolated and composite was regenerated through just changing the pH of aqueous solution and reusable at least 5 times without reasonable decrease in its efficiency (Fig. 2c & Fig. S26, Table S8, see ESI[†]). The synthesized composite is capable to decompose the adsorb dye and possible to regenerate for at least 5 times through photocatalytic degradation in water under UV light (Fig. 2d &Fig. S27-28, Table S9, see ESI[†]).

Thus, the adsorption efficiency synthesized nanocomposite is superior and possible to use for practical application as selective adsorbent for either cationic or anionic dyes from their mixture just by varying the pH and re-generable by desorption or photocatalytic degradation. The obtained selective adsorption efficiency of the synthesized nanocomposite is much high to that of other reported adsorbents (Table S10, see ESI[†]). Besides, most of the reported adsorbents can adsorb only one type of dye, not photodegradable and sometimes needs organic solvent for recovery of adsorbed dye.

In summary, we have successfully developed a novel synthetic strategy for the synthesis of fully exfoliated layered titanate-cationically functionalized amylopectin based composite through simultaneous *in-situ* layered titanate formation, exfoliation, and polymerization. The synthesized composite showed rapid and efficient pH responsive dye adsorption property. At lower pH, it adsorbs anionic dyes while at higher pH cationic dyes were adsorbed, selectively. The synthesized adsorbed composite is efficiently generated by desorption as well photocatalytic degradation and reusable at least five times without reasonable reduction of its adsorption efficiency. The developed procedure is extendable for the nanocomposite synthesis of fully exfoliated layer titanate as well as other inorganic layer material and any cationically functionalized natural or synthetic polymer. The nanocomposites can also be used in various applications other than adsorption and photocatalytic degradation.

Notes and references

Acknowledgement: CSIR-CSMCRI Communication No. 146/2015. Financial support from the DST, India (NO:DST/TM/WTI/2K12/67) is highly acknowledged. Instrumental facilities of CRF, ISM, Dhanbad and "ADCIF" of CSMCRI are also gratefully acknowledged. Authors are thankful to Dr. Biswajit Chowdhury, Department of Applied Chemistry, ISM, Dhanbad for his kind help towards surface area measurement.

1 W. Azim, R. K. Sani, U. C. Banerjee, Enzyme Microb. Technol. 1998, 22, 185−191;
2 I. Ali, Chem. Rev. 2012, 112, 5073−5091; G. Crini, Bioresour. Technol. 2006, 97, 1061−1085.
3 S. Deng, H. Xu, X. Jiang, J. Yin, Macromolecules 2013, 46, 2399−2406.
4 a) B. O. Okesola and D. K. Smith, Chem. Commun., 2013, 49, 11164–11166; b) N. Cheng, Q. Hu, Y. Guo, Y. Wang, and L. Yu, ACS Appl. Mater. Interfaces 2015, 7, 10258−10265;c) F. R.-Llansola, B. Escuder, J. F. Miravet, D. H.-Merino, I. W. Hamley, C. J. Cardin and W. Hayes, Chem. Commun., 2010, 46, 7960–7962; d) S. Deng, R. Wang, H. Xu, X. Jiang and J. Yin, J. Mater. Chem., 2012, 22, 10055–10061.
5 a) B. Li, X. Jiang and J. Yin, J. Mater. Chem., 2012, 22, 17976–17983; b) P. Zhang, J. Yin and X. Jiang, Langmuir, 2014, 30, 14597–14605; c) H. P. C. van Kuringen, G. M. Eikelboom, I. K. Shishmanova, D. J. Broer and A. P. H. J. Schenning, Adv. Funct. Mater., 2014, 24, 5045–5051; d) L.–L. Lv, J. Yang, H.-M. Zhang, Y.-Y. Liu and J.-F. Ma, Inorg. Chem. 2015, 54, 1744−1755.
6 a) X. Yan, S. Yao, Y. G. Li, Z. M. Zhang, Y. Lu, W. L. Chen and E. B. Wang, Chem.–Eur. J., 2014, 20, 6927–6933. b) Z. Zhu, Y. L. Bai, L. Zhang, D. Sun, J. Fang and S. Zhu, Chem. Commun., 2014, 50, 14674–14677; c) Y. Han, S. Sheng, F. Yang, Y. Xie, M. Zhao and J.-R. Li, J. Mater. Chem. A, 2015, 3, 12804–12809; d) F.-Y. Yi, W. Zhu, S. Dang, J.-P. Li, D. Wu, Y.-h. Li and Z.-M. Sun, Chem. Commun., 2015, 51, 3336—3339; e) W. Wei, R. Lu, H. Xie, Y. Zhang, X. Bai, L. Gu, R. Da and X. Liu, J. Mater. Chem. A, 2015, 3, 4314–4322.
7 a) C. Sarkar, C. Bora and S. K. Dolui, Ind. Eng. Chem. Res., 2014, 53, 16148–16155; b) H. Huang, J. Yu, W. Liu, and X. Jiang, NANO DOI: 10.1142/S1793292015500654;c) C.Gui, Q. Wang, S. Hao, J. Qu, P. Huang, C. Cao, W. Song and Z. Yu, *ACS Appl. Mater. Interfaces*, **2014**, *6*, 14653–14659; d) J. Ma, F. Yu, L. Zhou, L. Jin, M. Yang, J. Luan, Y. Tang, H. Fan, Z. Yuan and J. Chen, ACS Appl. Mater. Interfaces, 2012, 4, 5749–5760
8 a) N. Sutradhar, S. K. Pahari, M. Jayachandran, A. M. Stephan, J. R. Nair, B. Subramanian, H. C. Bajaj, H. M. Mody, A. B. Panda, *J. Mater. Chem. A*, 2013,*1*, 9122; b) N. Sutradhar, A. Sinhamahapatra, S. K. Pahari, H. C. Bajaj, A. B. Panda, ChemComm., **2011**, *47*, 7731; c) S. Xie, B. Zheng, Q. Kuang, X. Wang, Z. Xie and L. Zheng, CrystEngComm, 2012, 14, 7715–7720; d) P. Xiong, L. Wang, X. Sun, B. Xu, and X Wang, Ind. Eng. Chem. Res., 2013, 52, 10105–10113.
9 a) A. K. Sarkar, N. R. Mandre, A. B. Panda and S. Pal, *Carbohydr. Polym*. 2013, **95**, 753-759; b) A. K. Sarkar, A. Pal, S. Ghorai, N. R. Mandre and S. Pal, *Carbohydr. Polym.*, 2014, **111**, 108-115.
10 a) P.Gomez-Romero and C.Sanchez in Functional Hybrid Materials; Wiley VCH: Weinheim, Germany, **2004**, Chapters 1 and 8;b) J. P. Jose and S. Thomas, *Phys. Chem. Chem. Phys.*, 2014, **16**, 14730-14740; c) J. Low, S. Cao, J. Yu and S. Wageh, *Chem. Commun.*, 2014, **50**, d) 10768-10777; G. Keledi, J. Hári and B. Pukánszky, *Nanoscale*, 2012, **4**, 1919-1938.
11 S. Ghorai, A. Sarkar, M. Raoufi, A. B. Panda, H. Schönherr and S. Pal, *ACS Appl. Mater. Interfaces.,* 2014, **6**, 4766-4777.
12 O. Yoshida and M. Okamoto, *Macromol. Rapid Commun.*, 2006, **27**, 751-757.
13 a) Y. Fuse, Y. Ideb and M. Ogawa, *Polym. Chem*., 2010, **1**, 849-853;b)T. Guo, L. Wang, D. G. Evans and W. Yang, *J. Phys. Chem. C.*, 2010, **114**, 4765-4772; c) N. Sukpirom and M. M. Lerner. *Chem. Mater.*, 2001, **13**, 2179-2185.
14 X. Huang, D. Appelhans, P. Formanek, F. Simon, B. Voit, *ACS Nano,* 2012, **6**, 9718-9726.